

Electronic Supplementary Information

“Twisted” small molecule donors with enhanced intermolecular interactions in condensed phase towards efficient and thick-film all-small-molecule organic solar cells

Xiafei Cheng^{a, c}, *Ziqi Liang*^a, *Shifeng Liang*^a, *Xuwen Zhang*^a, *Jie Xu*^a, *Yan Xu*^a, *Wang Ni*^{b, *},
Miaomiao Li^{a, *}, *Yanhou Geng*^{a, d}

^a School of Materials Science and Engineering and Tianjin Key Laboratory of Molecular Optoelectronic Science, Tianjin University, Tianjin, 300072, China. E-mail: miaomiao.li@tju.edu.cn.

^b Science and Technology on Power Sources Laboratory, Tianjin Institute of Power Sources, Tianjin, 300384, China. E-mail: niwang@tju.edu.cn

^c Sinopec (Beijing) Research Institute of Chemical Industry Co., Ltd, Beijing, 100013, China.

^d Joint School of National University of Singapore and Tianjin University, International Campus of Tianjin University, Binhai New City, Fuzhou 350207, China.

* Corresponding author.

1. Instruments

^1H NMR and ^{13}C NMR spectra were recorded using a Bruker 400-MHz spectrometer in chloroform-d (CDCl_3) at 25 °C with tetramethylsilane (TMS) as internal reference. Elemental analysis was conducted on a FlashEA1112 elemental analyzer. Matrix-assisted laser desorption ionization time-of-flight (MALDI-TOF) mass spectra were measured by a Bruker/AutoflexIII Smartbean MALDI mass spectrometer with 2-[(2E)-3-(4-t-butylphenyl)-2-methylprop-2-enylidene]malononitrile (DCTB) as the matrix in a reflection mode. Differential scanning calorimetry (DSC) was conducted on a Q25 differential scanning calorimeter (TA Instruments) with a heating/cooling rate of 10 °C min^{-1} under nitrogen. UV-vis-NIR absorption spectra were obtained on a Shimadzu UV3600-plus spectrometer. Solution spectra were measured in CF with a concentration of 1×10^{-5} mol L^{-1} and films were prepared by spin-casting with CF as solvent. The optical bandgap was calculated according to absorption onset of films ($E_{\text{g}}^{\text{opt}} = 1240/\lambda_{\text{onset}}$ eV). Cyclic voltammetry (CV) measurements were carried out on a CHI660a electrochemical workstation at a scan rate of 100 mV s^{-1} . A glassy carbon with 1 cm diameter, a Pt wire and a saturated calomel electrode (SCE) were used as working electrode, counter electrode and reference electrode, respectively. NBu_4PF_6 (0.1 M) in anhydrous acetonitrile was used as electrolyte. The potential was calibrated by ferrocene/ferrocenium (Fc/Fc^+). The HOMO and LUMO energy levels were estimated by the equations: $E_{\text{HOMO}} = -(4.80 + E_{\text{onset}}^{\text{ox}})$ eV and $E_{\text{LUMO}} = -(4.80 + E_{\text{onset}}^{\text{re}})$ eV, in which $E_{\text{onset}}^{\text{ox}}$ and $E_{\text{onset}}^{\text{re}}$ are oxidation and reduction onsets versus the half potential of Fc/Fc^+ , respectively. Density functional theory (DFT) calculations were conducted by Gaussian 09 with a hybrid B3LYP correlation functional and 6-31G (d) basis set and the 2-ethylhexyl side chain was simplified as methyl group. In plane and out of plane GIWAXS of the thin films were measured by a Rigaku Smart Lab with Cu K_α source ($\lambda = 1.54056$ Å) in air. Photoluminescent (PL) spectra were recorded on a Hitachi F-7000 spectrometer. TEM images were acquired on a JEM-2100PLUS electron microscopy (JEOL) at a 200 kV accelerating voltage.

2. Materials and synthesis

All chemical raw materials were purchased from commercial sources and used without further purification. Anhydrous chloroform, toluene and triethylamine were distilled before use from Calcium hydride or sodium. N3 and PDINO was purchased from Derthon Optoelectronic Materials Science Technology Co., Ltd. DRTT-T was synthesized in our lab according to our previous work¹ and used for comparison. Organotin monomers **1** and Compounds **2** and **3** were synthesized according to the reported literature¹⁻³.

Compound **4**. To a reaction tube were added compound **1** (100.0 mg, 105.5 μmol), **2** (159.1 mg, 232.0 μmol), $\text{Pd}(\text{PPh}_3)_4$ (9.8 mg, 8.4 μmol) and anhydrous toluene (3.0 mL) in glove box. The mixture was stirred in a microwave reactor at a dynamic model (160 $^\circ\text{C}$, 200 W) for 1 hour. Then the reaction mixture was poured into water and extracted with CHCl_2 . The combined organic extracts were dried over anhydrous MgSO_4 . After evaporating the solvent, the residue was purified by column chromatography on silica gel with petroleum ether/dichloromethane (1:1, v/v) as eluent to afford the product as a red waxy solid (177.8 mg, 92%). ^1H NMR (CDCl_3 , 400 MHz): δ (ppm) = 10.05 (s, 2H), 8.34 (s, 2H), 7.79 (s, 2H), 7.31 (d, $J=3.6$ Hz, 2H), 7.30 (d, $J=3.6$ Hz, 2H), 7.23 (d, $J=3.6$ Hz, 2H), 6.90 (t, $J=3.6$ Hz, 4H), 6.85 (d, $J=3.2$ Hz, 2H), 2.90-2.80 (m, 12H), 1.72-1.62 (m, 4H), 1.58-1.55 (m, 2H), 1.48-1.21 (48H), 0.98-0.83 (m, 36H). ^{13}C NMR (100 MHz, CDCl_3): δ (ppm) 184.69, 146.87, 146.51, 146.43, 143.40, 141.34, 139.83, 139.75, 139.41, 139.37, 135.80, 135.77, 135.51, 134.64, 132.86, 131.80, 128.33, 128.22, 127.95, 126.51, 126.48, 125.72, 125.55, 125.51, 124.64, 123.88, 41.46, 41.26, 34.33, 34.27, 34.14, 32.50, 32.41, 30.16, 29.73, 28.91, 28.84, 25.73, 25.68, 25.48, 23.05, 23.01, 14.20, 14.13, 10.90, 10.77. MALDI-TOF: calcd. for $\text{C}_{100}\text{H}_{120}\text{O}_2\text{S}_{10}\text{Se}_2$: 1833.5; Found. 1832.5.

Compound **5**. **5** (447.3 mg, 84%) was obtained as a red waxy solid from **1** (250.0 mg, 263.6 μmol) and **3** (452.2 mg, 580.0 μmol) following the procedure for the synthesis of **4**. ^1H NMR (CDCl_3 , 400 MHz): δ (ppm) = 10.04 (s, 2H), 8.33 (s, 2H), 7.80 (s, 2H), 7.41 (d, $J=3.6$ Hz, 2H), 7.35 (d, $J=3.6$ Hz, 2H), 7.31 (d, $J=3.6$ Hz, 2H), 7.05 (d, $J=3.6$ Hz, 2H), 7.00 (d, $J=3.6$ Hz, 2H), 6.91 (d, $J=3.6$ Hz, 2H), 2.93-2.88 (m, 8H), 2.78 (d, $J=5.2$ Hz, 4H), 1.70-1.58 (m, 6H), 1.48-1.25 (48H), 0.99-0.85 (m, 36H). ^{13}C NMR (100 MHz, CDCl_3): δ (ppm) 184.74, 155.15, 154.80, 154.61, 143.35, 141.17, 141.09, 139.73, 139.52, 139.27, 139.09, 137.10, 135.32, 134.75, 132.49, 130.72, 130.60, 130.40, 128.92, 128.73, 127.80, 127.70, 127.61, 126.88, 124.28, 42.24, 42.03, 37.03, 37.00, 36.90, 32.47, 32.40, 28.94, 28.87, 25.67, 25.64, 25.45, 23.05, 23.03, 14.21, 14.18, 10.89, 10.78. MALDI-TOF: calcd. for $\text{C}_{100}\text{H}_{120}\text{O}_2\text{S}_6\text{Se}_6$: 2021.3; Found. 2020.3.

DRTT-2Se. A solution of compound **4** (200 mg, 109.1 μmol) and 3-ethyl-2-thioxothiazolidin-4-one (176.0 mg, 1.1 mmol) in dry CHCl_3 (11 mL) was degassed twice with argon followed by the addition of a few drops of triethylamine. Then the reaction mixture was stirred at 70 $^\circ\text{C}$ for 8 hours. The solvent was removed under reduced pressure and the residues were purified by column chromatography on silica gel with CHCl_3 as eluent and Concentrated to a saturated solution then added dropwise in methanol for precipitation. The solid was collected by filtration to afford the product as a dark red solid (191.9 mg, 83%). ^1H NMR (CDCl_3 , 400 MHz): δ (ppm) = 7.96 (s, 2H), 7.92 (s, 2H), 7.76 (s, 2H), 7.31 (d, $J=3.6$ Hz, 2H), 7.29 (d, $J=3.6$ Hz, 2H), 7.24 (d, $J=3.6$ Hz, 2H), 6.91-6.88 (m, 6H), 4.21 (q, $J=7.2$ Hz, 4H), 2.89 (t, $J=6.8$ Hz, 8H), 2.84-2.82 (m, 4H), 1.72-1.68 (m, 4H), 1.58-1.55 (m, 2H), 1.48-1.25 (m, 54H), 0.98-0.86 (m, 36H). ^{13}C NMR (100 MHz, CDCl_3): δ (ppm) 192.35, 167.15, 154.53, 146.66, 146.46, 141.51, 140.03, 139.49, 138.69, 138.17, 138.06, 137.19, 136.08, 135.95, 132.63, 131.71, 130.40, 128.69, 128.22, 127.54, 125.93, 125.65,

125.21, 124.10, 123.66, 42.03, 41.47, 39.95, 36.92, 34.42, 34.29, 32.57, 32.53, 32.43, 29.73, 28.96, 28.93, 28.89, 25.79, 25.73, 25.47, 23.09, 23.07, 23.02, 14.22, 14.21, 14.16, 12.29, 10.99, 10.91, 10.76. MALDI-TOF: calcd. for $C_{110}H_{130}N_2O_2S_{14}Se_2$: 2119.5; Found. 2118.5. Elemental Anal. Calcd.: C 62.35, H 6.18, N 1.32, S 21.18; Found: C 61.93, H 6.32, N 1.45, S 20.89.

DRTT-6Se. DRTT-6Se (277.5 mg, 81%) was obtained as a dark red solid from **5** (300.0 mg, 148.5 μ mol) and 3-ethyl-2-thioxothiazolidin-4-one (239.4 mg, 1.5 mmol) following the procedure for the synthesis of DRTT-2Se. 1H NMR ($CDCl_3$, 400 MHz): δ (ppm) = 7.96 (s, 2H), 7.91 (s, 2H), 7.77 (s, 2H), 7.40 (d, $J=3.6$ Hz, 2H), 7.36 (d, $J=3.6$ Hz, 2H), 7.30 (d, $J=3.6$ Hz, 2H), 7.03 (m, 4H), 6.91 (d, $J=3.6$ Hz, 2H), 4.21 (q, $J=7.2$ Hz, 4H), 2.93 (t, $J=6.8$ Hz, 8H), 2.84-2.82 (m, 4H), 1.68-1.65 (m, 4H), 1.58-1.55 (m, 2H), 1.47-1.27 (m, 54H), 0.99-0.87 (m, 36H). ^{13}C NMR (100 MHz, $CDCl_3$): δ (ppm) 192.40, 167.17, 154.94, 154.80, 154.52, 141.42, 141.36, 141.34, 139.87, 139.48, 138.66, 138.03, 137.94, 137.19, 135.91, 132.64, 131.84, 130.58, 130.52, 130.37, 128.73, 127.75, 127.57, 127.46, 126.34, 126.00, 124.25, 123.63, 42.24, 42.22, 42.02, 39.96, 37.13, 37.00, 36.92, 32.54, 32.50, 32.43, 28.96, 28.94, 28.88, 25.79, 25.68, 25.47, 23.07, 23.05, 23.02, 14.22, 14.20, 14.16, 12.29, 10.96, 10.89, 10.77. MALDI-TOF: calcd. for $C_{110}H_{130}N_2O_2S_{10}Se_6$: 2309.2; Found. 2308.2. Elemental Anal. Calcd.: C 57.28, H 5.68, N 1.21, S 13.90; Found: C 56.64, H 5.83, N 1.43, S 14.17.

3. Fabrication and characterization of OSC devices (*J-V*, EQE, FTPS-EQE, TPV, TPC)

OSC devices with a conventional architecture of ITO/PEDOT:PSS (30 nm)/active layer/PDINO (10 nm)/Al (100 nm) or Ag (150nm) were fabricated with CF as solvent. ITO was cleaned ultrasonically with soap deionized water, deionized water, acetone and isopropanol for 10 min, successively. The dried ITO was treated with UV-ozone for 25 min. Then a solution of PEDOT:PSS (Baytron PVP Al4083) was spin-coated on the surface at a spinning rate of 4500 r.p.m. for 20 s. After baking at 140 °C for 20 min, the substrates were transferred into glovebox under N_2 atmosphere. The active layer solution was prepared in chloroform and then stirred at 30 °C at least 3 hours. The blend solution was subsequently spin-coated on the PEDOT:PSS layer to form an active layer. The active layers with thickness of ~120, ~150, ~220 and ~300 nm were spin-coated from the chloroform solution (total concentration: 25 mg ml^{-1}) at 3000, 2000, 1000 and 500 r.p.m., respectively. The thickness of the active layer was measured by Dektak 150 profilometer, and the average thickness was obtained from over 6 values. Further on, the thin films were thermally annealed at different temperatures and in different ways. Then, PDINO in methanol solution was deposited on the active layer to give an interfacial layer. Al (ca. 100 nm) or Ag (ca. 150 nm) top electrode was subsequently deposited on the PDINO layer under high vacuum ($< 1.5 \times 10^{-4}$ Pa). Keithley 2400 source meter was used to measure *J-V* curves under 100

mW cm⁻² AM 1.5G simulated solar light illumination provided by a Solar Simulator (SS-F5-3A, Enli Technology Co. Ltd) calibrated with a standard photovoltaic cell equipped with a KG5 filter in a glove box. The EQE curves were recorded by the integrated quantum efficiency measurement system QE-R (Enli Technology Co. Ltd., Taiwan), which was calibrated with a crystal silicon photovoltaic cell ahead of the measurement. The FTPS-EQE measurement was carried out on an Enlitech FTPS PECT-600 instrument. Transient photocurrent (TPC) and photovoltage (TPV) measurements were performed on a Moxel 180081-4320 with light intensity about 0.5 sun. Voltage and current dynamics were recorded on a digital oscilloscope (Tektronix MDO4104C). Voltages at open circuit and currents under short circuit conditions were measured over a 1 MΩ and a 50 Ω resistor, respectively.

4. SCLC measurement

The hole/electron mobility was measured using the space charge limited current (SCLC) method. Hole-only and electron-only devices were fabricated with architecture of ITO/PEDOT:PSS (30 nm)/active layer or neat donor film (~120 nm)/Au (100 nm) and ITO/ZnO (30 nm)/active layer (~120 nm)/Al (100 nm), respectively. The devices were measured using Keithley 2400 source meter in the dark and the mobilities were obtained by taking current-voltage curves and fitting the results to a space charge limited form, where the SCLC is described by:

$$J = \frac{9}{8} \varepsilon_0 \varepsilon_r \mu \frac{V^2}{L^3}$$

Where J is the current density, L is the thickness of the film, μ is the hole or electron mobility, ε_0 is the permittivity of free space, ε_r is the relative permittivity of the material (assumed to be 3), V ($= V_{\text{appl}} - V_{\text{bi}}$) is the internal voltage in the device, where V_{appl} is the applied voltage, V_{bi} is the built-in voltage (0 V), V_{rs} is the voltage drop from the substrate's series resistance ($V_{\text{rs}} = IR$, R is measured to be 10.8 Ω).

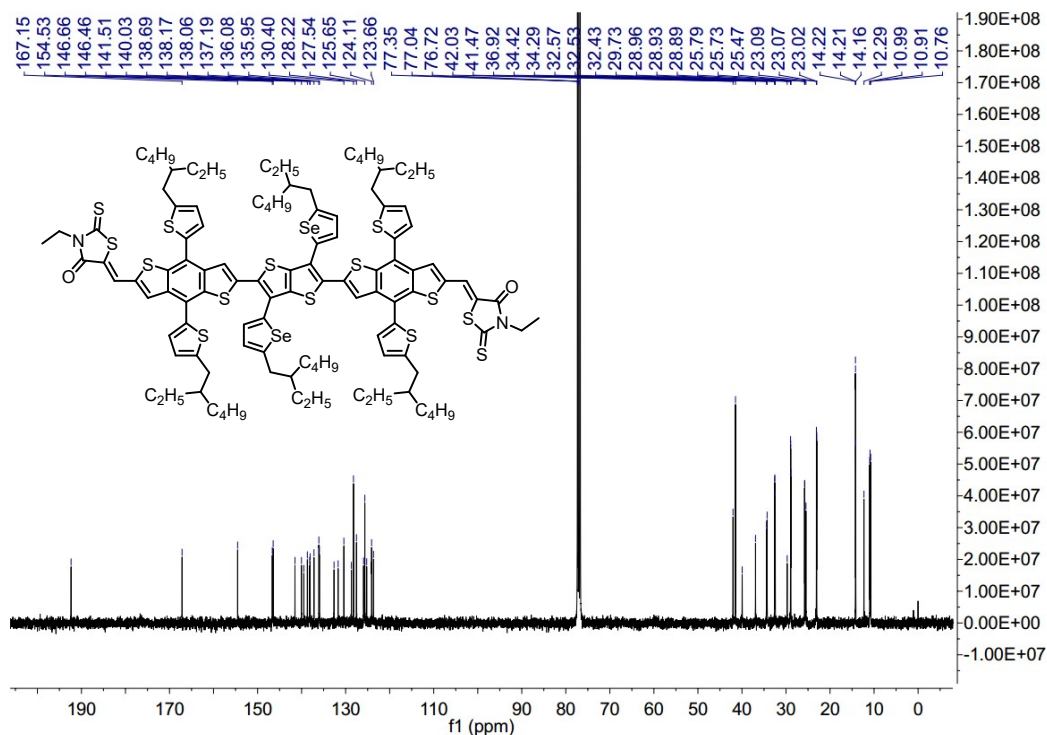


Fig. S3 ¹³C NMR spectrum of DRTT-2Se.

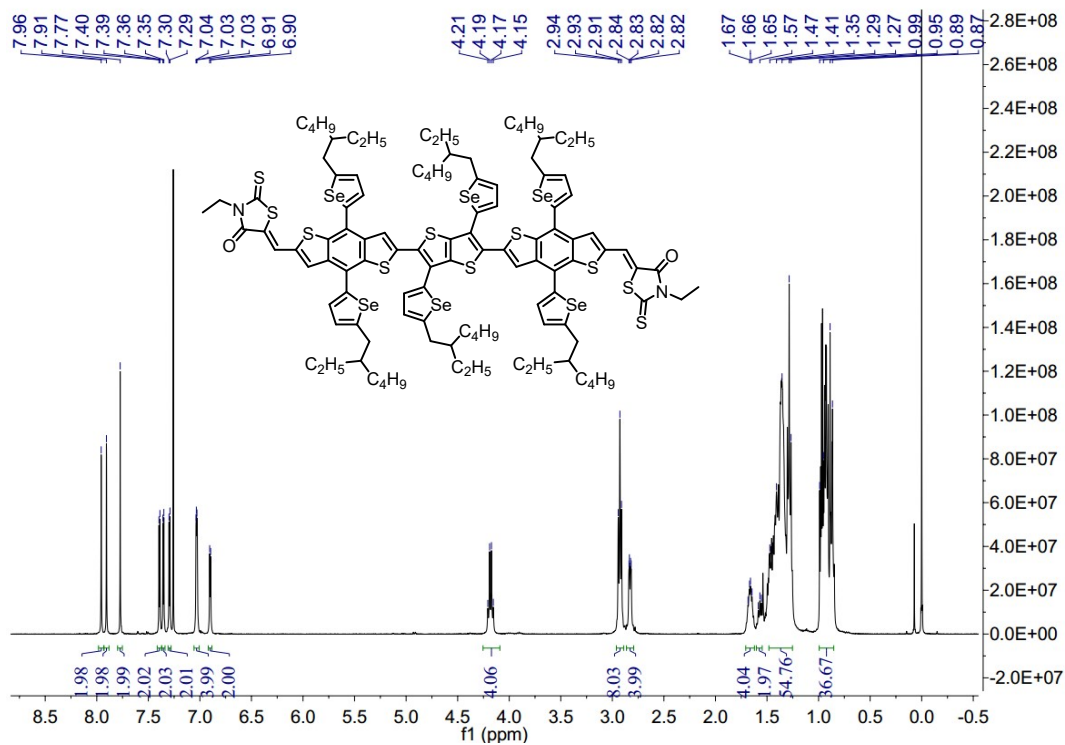


Fig. S4 ¹H NMR spectrum of DRTT-6Se.

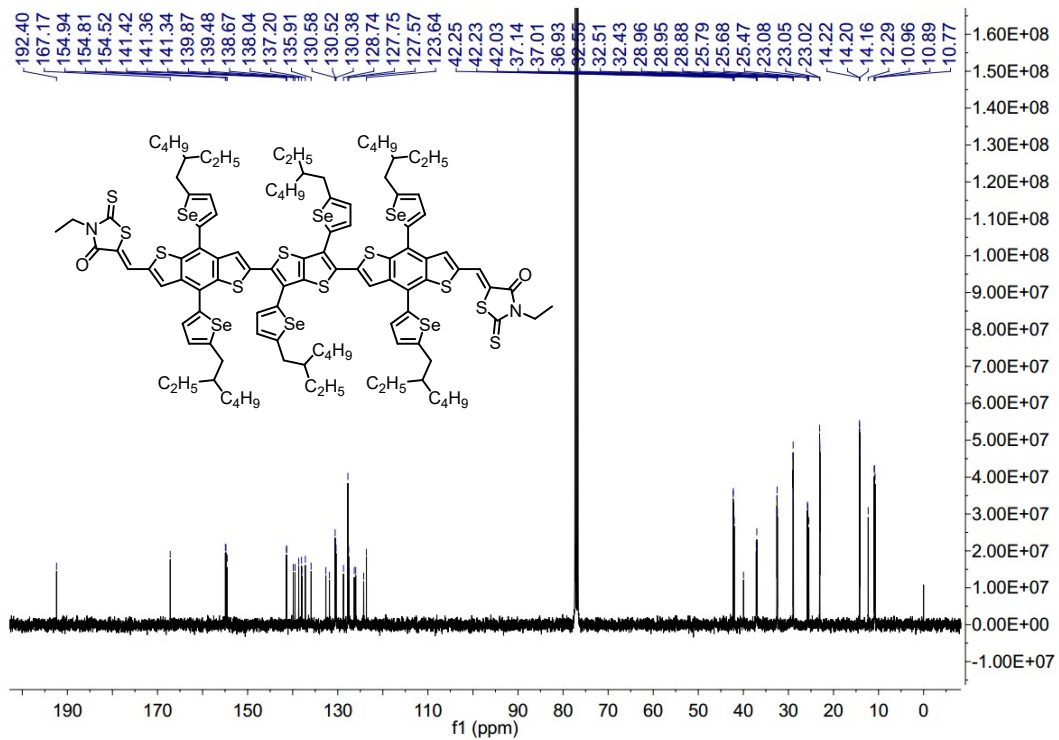


Fig. S5 ^{13}C NMR spectrum of DRTT-6Se.

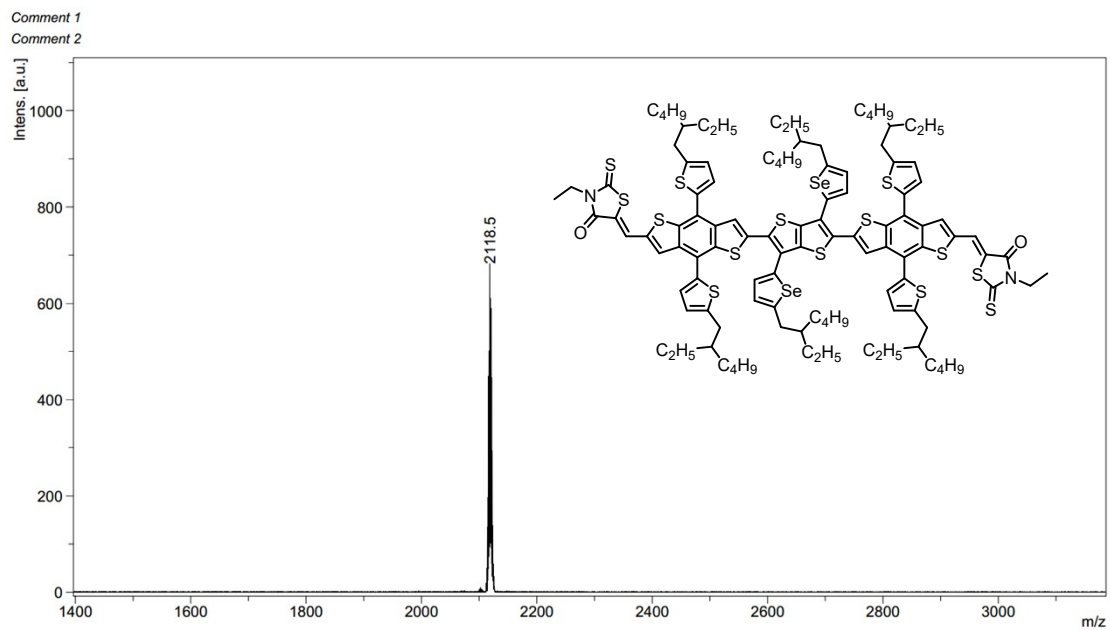


Fig. S6 The MALDI-TOF mass spectrum of DRTT-2Se.

Comment 1
Comment 2

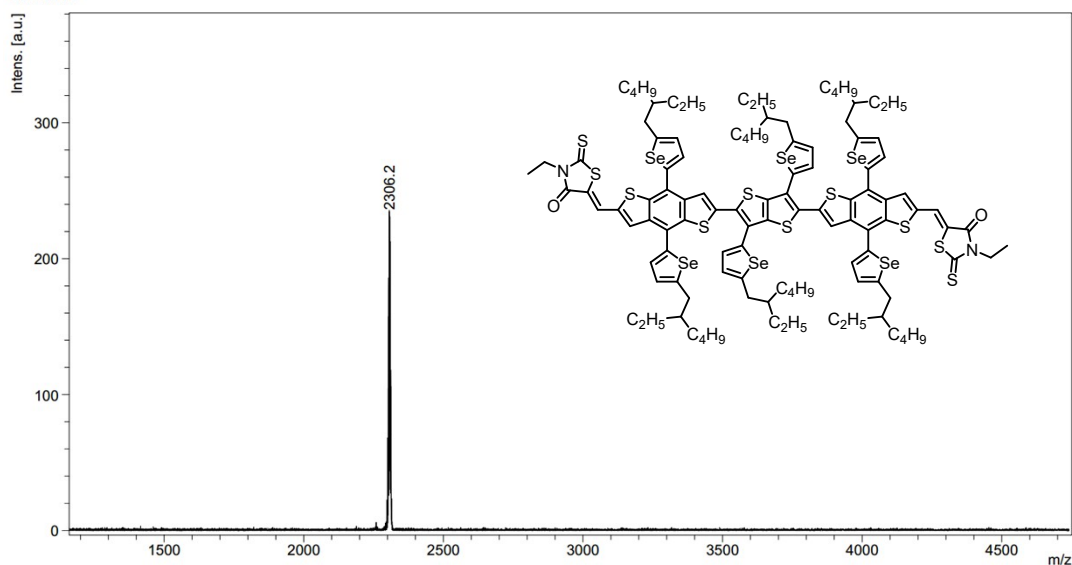


Fig. S7 The MALDI-TOF mass spectrum of DRTT-6Se.

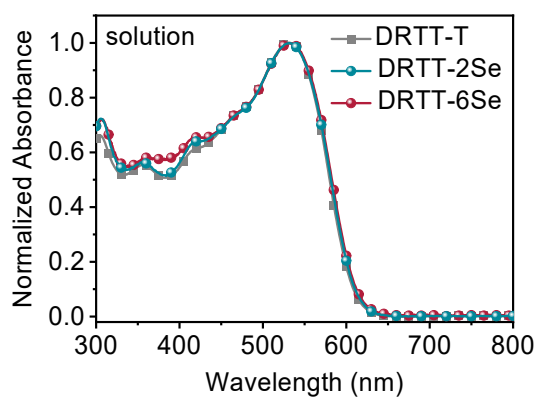


Fig. S8 Absorption spectra of DRTT-T, DRTT-2Se and DRTT-6Se in chloroform solutions (10^{-5} mol/L in chloroform).

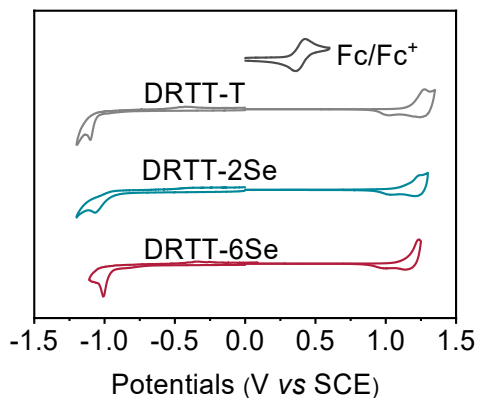


Fig. S9 Thin film cyclic voltammograms (CV) of DRTT-T, DRTT-2Se and DRTT-6Se.

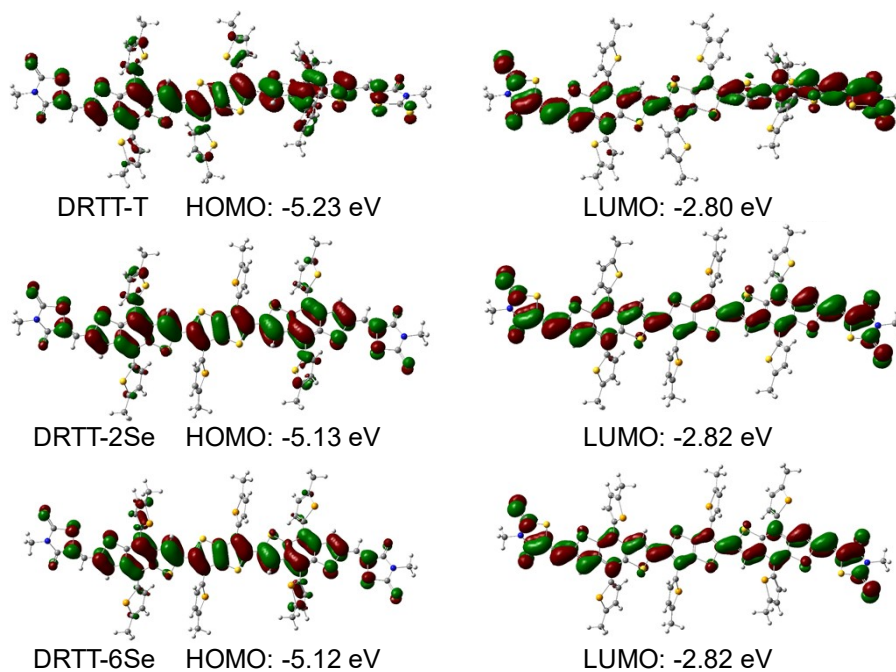


Fig. S10 DFT-calculated frontier orbitals of the molecules (long alkyls replaced by methyl groups).

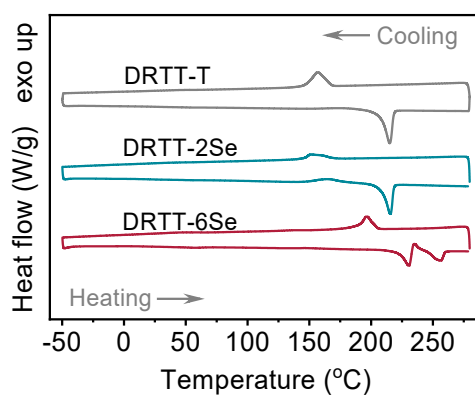


Fig. S11 Differential scanning calorimetry (DSC) thermograms of the donor molecules at a scan rate of 10 °C min⁻¹.

Table S1 Thermodynamic parameters of DR TT-T, DR TT-2Se and DR TT-6Se.

molecule	T_m [°C]	ΔH_m [J/g]	T_c [°C]	ΔH_c [J/g]
DR TT-T	215.0	29.0	156.4	20.4
DR TT-2Se	215.6	23.6	151.2	9.6
DR TT-6Se	230.7 256.4	13.4, 10.3	196.3	16.7

Table S2 Out-of-plane and in-plane XRD data and μ_h of DRTT-T, DRTT-2Se and DRTT-6Se neat films with TA treatment.

	<i>out-of-plane</i>				<i>in-plane</i>		μ_h^a ($10^{-4} \text{ cm}^2 \text{ V}^{-1} \text{ s}^{-1}$)
	(100)		(010)		(100)		
	d-spacing (Å)	CCL (Å)	d-spacing (Å)	CCL (Å)	d-spacing (Å)	CCL (Å)	
DRTT-T	20.37	195.82	3.66	35.07	21.55	184.30	2.32 (2.11)
DRTT-2Se	20.62	178.31	3.66	40.72	21.62	210.17	3.36 (3.12)
DRTT-6Se	20.99	183.25	3.64	37.61	21.75	201.80	3.70 (3.56)

^a Optimal and statistical results are listed outside of parentheses and in parentheses, respectively. The average values are obtained from over 10 devices.

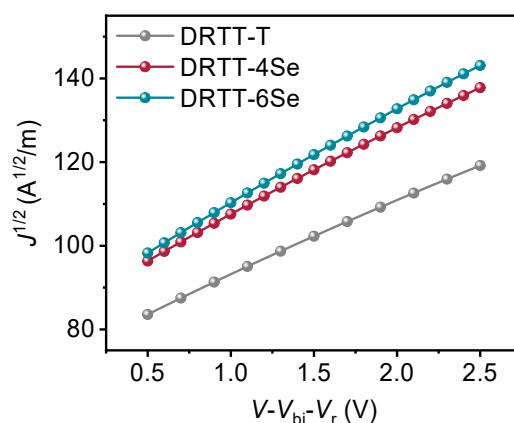


Fig. S12 J - V characteristics for the hole-only devices based on DRTT-T, DRTT-2Se and DRTT-6Se neat films. The solid lines represent the fit using a model of single carrier SCLC with field-independent mobility.

Table S3 The detailed photovoltaic performance of OSCs based on DRTT-2Se:N3 and DRTT-6Se:N3 with Al as top electrode upon different TA treatment.

donor	TA temperature (°C)	V_{oc}^a (V)	J_{sc}^a ($\text{mA} \cdot \text{cm}^{-2}$)	FF ^a (%)	PCE ^a (%)
DRTT-2Se	As cast	0.88 (0.87±0.01)	16.47 (16.17±0.46)	46.3 (45.8±0.9)	6.68 (6.45±0.17)
	70-130 ^b	0.86 (0.85±0.01)	23.75 (23.22±0.51)	68.5 (67.8±0.5)	13.95 (13.44±0.26)
DRTT-6Se	As cast	0.89 (0.89±0.00)	16.98 (16.54±0.38)	50.9 (50.2±0.6)	7.68 (7.52±0.14)
	110	0.85 (0.85±0.00)	21.12 (20.75±0.23)	70.7 (70.1±0.4)	12.74 (12.52±0.15)
	120	0.84 (0.84±0.00)	24.08 (23.65 ±0.27)	69.3 (68.9±0.3)	14.09 (13.88±0.16)

130	0.84 (0.84±0.00)	23.35 (22.78±0.43)	64.3 (63.6±0.5)	12.59 (12.26±0.21)
-----	---------------------	-----------------------	--------------------	-----------------------

^a Optimal and statistical results are listed outside of parentheses and in parentheses, respectively. The average values are obtained from over 10 devices. ^b The two-step TA was conducted with 70 °C for 2 min then 130 °C for 50 s.

Table S4 The detailed photovoltaic performance of DRTT-2Se:N3- and DRTT-6Se:N3-based OSCs with different D/A ratio (Al as the top electrode).

donor:N3	D/A	V_{OC}^a (V)	J_{SC}^a (mA·cm ⁻²)	FF ^a (%)	PCE ^a (%)
DRTT-2Se	1/0.6	0.84 (0.84±0.01)	24.42 (23.84±0.47)	67.2 (66.7±0.4)	13.81 (13.32±0.29)
	1/0.75	0.86 (0.85±0.01)	23.75 (23.22±0.51)	68.5 (67.8±0.5)	13.95 (13.44±0.26)
	1/0.9	0.85 (0.85±0.00)	23.16 (22.65±0.44)	64.3 (63.7±0.4)	12.59 (12.33±0.18)
DRTT-6Se	1/0.5	0.84 (0.84±0.01)	22.94 (22.72±0.19)	71.2 (70.7±0.4)	13.72 (13.59±0.11)
	1/0.6	0.84 (0.84±0.01)	23.69 (23.34±0.30)	71.0 (70.2±0.7)	14.21 (14.06±0.12)
	1/0.75	0.84 (0.84±0.00)	24.08 (23.65±0.27)	69.3 (68.9±0.3)	14.09 (13.88±0.16)
	1/0.9	0.85 (0.85±0.00)	22.58 (22.28±0.21)	69.0 (68.1±0.6)	13.19 (13.00±0.13)

^a Optimal and statistical results are listed outside of parentheses and in parentheses, respectively. The average values are obtained from over 10 devices.

Table S5 The detailed photovoltaic performance of optimized DRTT-T:N3-, DRTT-2Se:N3- and DRTT-6Se:N3-based OSCs with Al as the top electrode .

donor:N3	V_{OC}^a (V)	J_{SC}^a (mA·cm ⁻²)	FF ^a (%)	PCE ^a (%)
DRTT-T ^b	0.85 (0.85±0.01)	23.87 (23.20±0.34)	65.1 (64.7±0.6)	13.21 (12.84±0.27)
DRTT-2Se ^b	0.86 (0.85±0.01)	23.75 (23.22±0.51)	68.5 (67.8±0.5)	13.95 (13.44±0.26)
DRTT-6Se ^d	0.84 (0.84±0.01)	23.69 (23.34±0.30)	71.0 (70.2±0.7)	14.21 (14.06±0.12)

^a Optimal and statistical results are listed outside of parentheses and in parentheses, respectively. The average values are obtained from over 10 devices. ^b The two-step TA was conducted with 70 °C for 2 min then 130 °C for 50 s. ^c The one-step TA was conducted with 120 °C for 10 min.

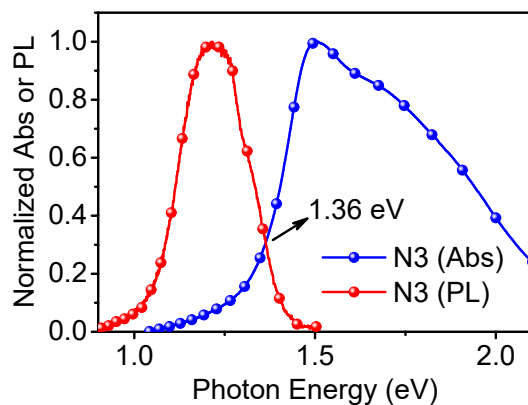


Fig. S13 Details of optical E_g determination. E_g is estimated by the cross-point of normalized absorption (blue line) and photoluminescence (PL) spectra (red line) of the N3 neat film, being 1.36 eV for N3.

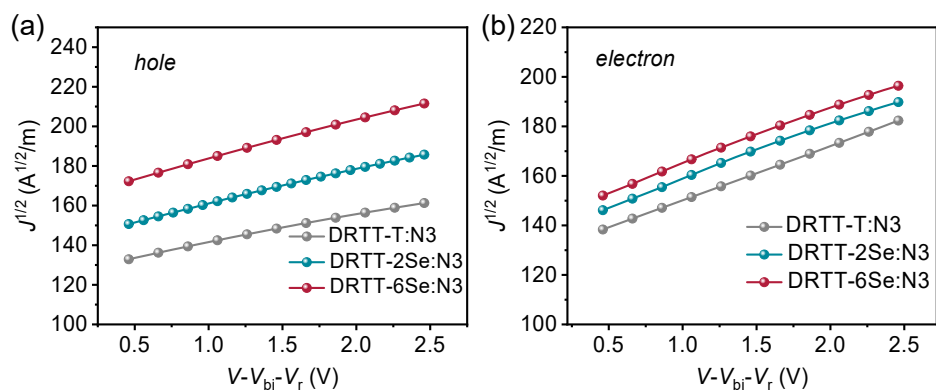


Fig. S14 J - V characteristics for the hole-only (a) and electron-only (b) devices based on DRTT-T:N3, DRTT-2Se:N3 and DRTT-6Se:N3. The solid lines represent the fit using a model of single carrier SCLC with field-independent mobility.

Table S6 Mobility results of SCLC devices based on donor:N3 blend films.

	μ_h^a ($10^{-4} \text{ cm}^2 \text{ V}^{-1} \text{ s}^{-1}$)	μ_e^a ($10^{-4} \text{ cm}^2 \text{ V}^{-1} \text{ s}^{-1}$)	μ_h/μ_e
DRTT-T:N3	1.17 (1.05)	2.78 (2.65)	0.42
DRTT-2Se:N3	1.79 (1.68)	2.83 (2.70)	0.63
DRTT-6Se:N3	2.24 (2.11)	2.89 (2.77)	0.78

^a Optimal and statistical results are listed outside of parentheses and in parentheses, respectively. The average values are obtained from over 10 devices.

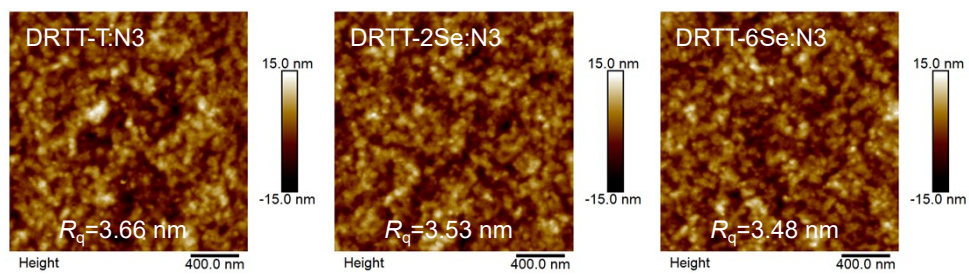


Fig. S15 AFM images of DRTT-T:N3, DRTT-2Se:N3 and DRTT-6Se:N3 blend films with TA treatments.

References

1. X. Cheng, M. Li, Z. Guo, J. Yu, G. Lu, L. Bu, L. Ye, H. Ade, Y. Chen and Y. Geng, *J. Mater. Chem. A*, 2019, **7**, 23008–23018.
2. W.-H. Chang, L. Meng, L. Dou, J. You, C.-C. Chen, Y. Yang, E. P. Young, G. Li and Y. Yang, *Macromolecules*, 2015, **48**, 562-568.
3. Y. J. Kim, J. Y. Baek, J.-j. Ha, D. S. Chung, S.-K. Kwon, C. E. Park and Y.-H. Kim, *J. Mater. Chem. C*, 2014, **2**, 4937-4946.